

© 2020. A. Malewski, M. Kozłowski, W. Sumelka, M. Poledniok.

This is an open-access article distributed under the terms of the Creative Commons Attribution-NonCommercial-NoDerivatives License (CC BY-NC-ND 4.0, <https://creativecommons.org/licenses/by-nc-nd/4.0/>), which permits use, distribution, and reproduction in any medium, provided that the Article is properly cited, the use is non-commercial, and no modifications or adaptations are made.



# LARGE SCALE ARCHITECTURAL GLASS SLUMPING PROCESS - CHALLENGES AND LIMITATIONS

A. MALEWSKI<sup>1</sup>, M. KOZŁOWSKI<sup>2</sup>, W. SUMELKA<sup>3</sup>, M. POŁEDNIOK<sup>4</sup>

The paper focuses on the development of knowledge about the hot bending of curved architectural glass produced by the slumping process and the challenges as well as the limitations thereof. Due to the complexity of the process, many factors influence the final quality of the glass and the main objective was to better understand the procedure itself in order to improve the control and quality of the slumping process. As a result of the growing interest in this type of glass for architectural applications, the glass processing market is increasingly investing in the required technology. For the moment, this growing niche does not have a large number of direct explanations of the glass behaviour in the furnace in the available literature, which in turn encourages cooperation between the scientific community and manufacturers. This paper presents the conducted experiments that have led to a better understanding of the furnace's work and the impact of specific factors on its operation. Based on the 3D numerical model, a large sample of glass was produced, which was then scanned with a 3D laser using a method developed for the experiment. The results suggested that a more accurate test with usage of a full-size furnace is required. Based on this, the experiment was carried out using a large number of glass samples of different thicknesses. The results of the experiment helped to better understand and demonstrate the need for further research of this technology in order to optimize the quality of the process.

*Keywords:* glass formation, curved glass, modern architecture, glass production, laser scanning, glass behaviour

<sup>1</sup> M.Sc., Eng., Poznan University of Technology, Institute of Structural Analysis, Piotrowo 5, 60-965 Poznan, Poland, e-mail: andrzej.n.malewski@doctorate.put.poznan.pl

<sup>2</sup> DSc., PhD., Eng., Silesian University of Technology, Department of Structural Engineering, Akademicka 5, 44-100 Gliwice, Poland, e-mail: marcin.kozlowski@polsl.pl

<sup>3</sup> DSc., PhD., Eng., Prof. PUT, Poznan University of Technology, Institute of Structural Analysis, Piotrowo 5, 60-965 Poznan, Poland, e-mail: wojciech.sumelka@put.poznan.pl

<sup>4</sup> Process Engineer, Press Glass S.A, ul. 100, Cielmicka 44, Tychy, Poland, e-mail: marek.poledniok@pressglass.com

## 1. INTRODUCTION

Building façade has always been a hallmark of the owner as well as a design team, where usage of the glass was one of most important considerations [1]. The constant development of design and engineering tools e.g. Finite Element Analysis (FEA) in connection with non-uniform rational basis spline (NURBS) modelling allows to create more advanced geometries and enhance a new area of free-form building elements. Therein, glass plays one of the main roles and architects are consistently reaching for new methods of glass production [2] to stand out and distinguish their designs among others and one of these is free-form curved glass which is allowing to add spatial effects to facades. Forming glass is widely known and established technology in many industries such as automotive, optics or marine ([3], [4], [5]). However, during years an increase interest for large scale, free-form units for architectural purposes can be observed. This is reflected in the number of papers in the topic to explore such as ([6], [7], [8]), which are focused on describing area of architectural usage that has been mentioned before. Similar topics are also presented on the glass related conferences worldwide like annual International Conference on Advanced Building Skins in Bern [9], all other well-known conferences like Challenging Glass Conference [10], Advances in Architectural Geometry [11] or Design Modelling Symposium taking place in Berlin [12]. Free form shape of building envelope can be developed by a tessellated number of glass units, which all together results in the final geometry of the facade ([13] [14] [15]). Good examples are Bálua Budapest in Budapest (Fig. 1a) or Prada Aoyama in Tokyo (Fig. 1b). Another interesting example can be the renovation project Nordstan Shopping Centre, where the old facade has been replaced by insulated glass units (IGUs) with a wavy pattern (Fig. 2).



Fig. 1 a) Mixed Use Development Balna in Budapest by ONL (source: <https://www.oosterhuis.nl/>) b) Prada Aoyama in Tokyo by Herzog and de Meuron (source: <https://www.herzogdemeuron.com/>)



Fig. 2 - Renovation of Nordstan Shopping Centre facade in Sweden

Architects can freely generate desired geometry which can be adapted to existing building as results of the renovation e.g. Queen Elizabeth II Great Court at the British Museum [16] or new building such as Glass Entrance Van Gogh Museum in Amsterdam [10]. The form of the pieces, however, is limited by numerous factors such as type of curvature like single or double, geometrical shape, dimensions of a single unit, geometry related issues like magnitude of concave or convex surfaces which can be achieved by bending process, fixation methods or costs associated with proposed solutions [17]. It is worth to mention that installation aspects need to be also taken into account like customized equipment required for handling on the construction site (curved surface requires adjustable suction devices). These customized requirements, which are not standard, also increase costs during installation. From the perspective of production possibilities, several methods are being currently used to shape the glass sheets. One of the most popular is gravitational bending commonly named as "slumping" which allows to bend in one plane when the heated glass deforms on a table with an adjustable radius [18], [19]. It is also possible to bend in many planes (free form), when the glass sinks into a specially prepared form (e.g. by CNC milling from 3D model) and takes on its shape. Second one is forced shaping by pressing a glass against customized form into the desired shape [20]. There is also a cold bending method of laminated glass [21], however limited shape and curvature of the glass can be achieved, but will not be discussed further in this work. The slumping process is the one that is currently further developed for architectural glass production and is the subject of our research. It should be pointed out that there is a number of issues which still has to be further investigated to call gravitational bending process efficient and repeatable. Each single ply must be produced within tight tolerances ( $\pm$  couple of millimetres) which is needed to align single units on the facade and must be even more restrictive than a flat glass. These issues are even more

crucial during the production of laminated glass where each single ply needs to be laminated using e.g. polyvinyl butyral (PVB) foil as an interlayer and later be assembled as an insulated glass unit (IGU). The reason is that during the production these minor deviations can lead to lower visual aspects of final facade or contribute to decreasing durability of the product. Another significant factor is the lack of the possibility of thermal strengthening (tempering) of this type of glass, which translates into lower load capacity and sensitivity to thermal stress. The current study contributes to development of the knowledge regarding large scale glass slumping process and its limitation. It is focused on the experimental testing of free-form glass panes produced by glass slumping in industrial scale furnace. Moreover, the paper summarizes findings how sagging process is developing in the furnace and what limitations are to be considered during production in order to increase the quality of final product. Based on a Rhino model, a large sample of free-form glass pane was produced using a standard slumping process. Then, the sample was measured with 3D laser scanning methodology which has been investigated for this purpose. Discrepancies between 3D model and the obtained measurements were found which led to conclusions that more detailed experiments are required to better understand the phenomena behind the glass slumping. Therefore, an extensive experimental campaign was designed and conducted. It involved free slumping of small glass samples with different thicknesses. The structure of this paper is considered in such a way that it is first part materials, equipment and software used in the experiment to process the obtained data are characterised. Next, the methodology of 3D scanning with a laser scanner was described, together with its parameters and how to prepare the described materials for analysis. Next part is to describe the results and their interpretation. First a larger sample was measured, which allowed for the observation of differences requiring deeper investigations. In following, the experiment itself is further described in small details, as well as the analysis of how the geometry of the samples subjected to the experiment was changed as a result. At the end the outcomes are summarized showing both challenges and limitations.

## **2. MATERIALS AND METHODS**

### **2.1. MATERIALS, EQUIPMENT AND SOFTWARE**

For testing, glass samples were used of a thickness corresponding to that of the most commonly used soda–lime–silica glass in the building industry and each sheet was cut to 500 mm × 200 mm. The total number of samples in the test was 30 (Fig. 3a). As material it was used annealed glass i.e. without any residual stresses introduced by tempering that increases its load-bearing capacity. During testing,

the samples were placed on supports made of ceramic fibreboard, which is resistant to high temperatures and retains its dimensions during testing (negligible shrinkage). One of the most important elements of the test was the furnace used and its possibilities. The customized furnace consists of the main chamber on a near-square-plan with side dimensions exceeding 3 meters. Heating elements in the form of electric coil heaters are placed on a sliding furnace cover, where each of the heaters is equipped with a thermocouple which allows for individual temperature control and accurate operation of the furnace. It is worth mentioning that the furnace has no forced air circulation, i.e. it is not equipped with fans or other devices allowing to equalize the temperature in the oven and increase the heat exchange in the whole volume of the furnace. During the tests, the temperature inside the furnace was also measured in various places through 6 thermocouples. These were connected to multi-controller Simex MultiCon CMC-99 which was logging the signals each 30 seconds. A 3D Scanner Surphaser 100HSX was used to measure the surface of the sheets after the test, allowing the following measurements with scan rate of up to 1 million points per second (Fig. 3b). The results obtained have been further processed by application SurphExpress [22] provided by the manufacturer which allowed the results to be exported to 3D point cloud and mesh processing software CloudCompare [23]. This software helped to further process the results, such as cleaning the point cloud and comparing it to an assumed 3D model.

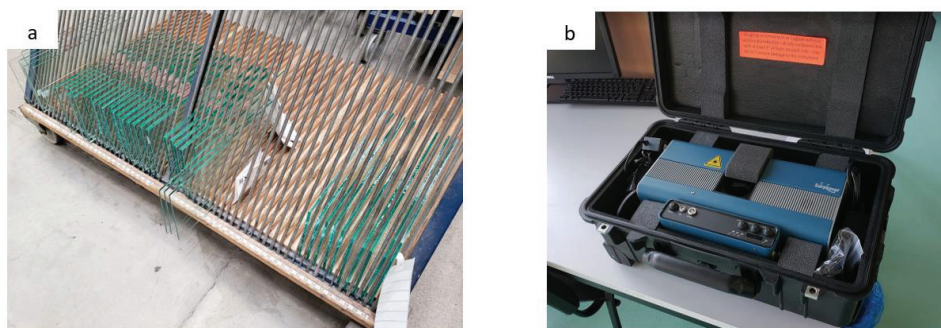


Fig. 3 a) Glass samples at racks b) 3D laser scanner SURPHASER 100HSX used for the experiment

## 2.2. 3D LASER SCANNING - METHODOLOGY

Basic challenge was to conquer obstacle of glass being completely transparent for laser beam and having high reflective surface which is known issue for laser scanners [24]. There are various methods of making glass surface opaque like using painting, talc spray or masking tape. Here, two latter types of surface pre-treatment were applied. At Poznan University of Technology glass was scanned with 3D laser scanner SURPHASER 100HSX Fig. 3b and this device was used for all further tests. Fig. 4a presents a sample covered with white technical talc spray (left part) and corresponding isolated point cloud (right part) obtained from 3D laser scanning with amount of 1.3M points collected by this particular measurement. The sample was about 1.5 m away from the scanner and each measurement was done individually. In order to check how the various surfaces affect the scanning results, the sample has been covered with technical talc of various thicknesses. In the top left corner, a square has been created which is 100% covered so that it is completely opaque. In the lower right corner, another square has been prepared this time covered with grey talc. The remaining part of the sample has been covered with talc in a sufficient way, i.e. places where the talc had a thinner layer and let the light through were allowed.

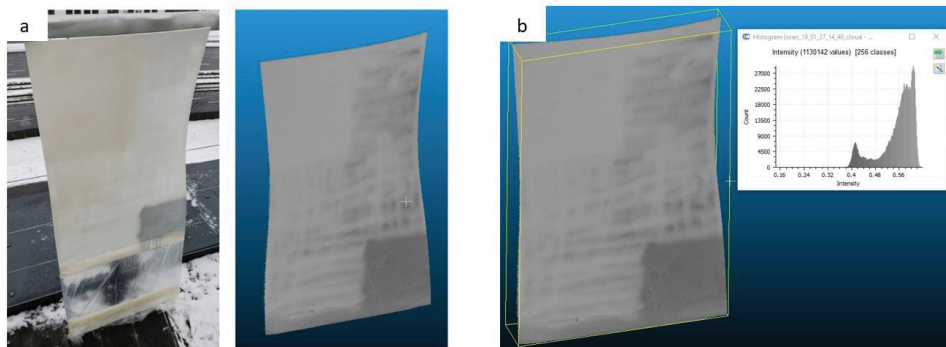


Fig. 4 a) Prepared sample with sprayed talc (on the left) and isolated point cloud from the 3D scan in CloudCompare (on the right) b) Intensity of scanned point cloud shown as grey-scale in CloudCompare software for single glass sample

Fig. 4b presents histogram of intensity and renders the same sample in grey scale which explains various quality of scanner readings. Intensity is the value that the laser measures together with the distance measurement and is the evaluation of the optical power of the reflected signal [24]. The graph to the right shows a histogram which counts the number of measured points on the vertical axis

and gives the intensity of each point on the horizontal axis. It is clear that grey is absorbing more of beam energy, therefore reflected signal intensity is lower. Dense white area (upper left corner) exposes naturally the highest intensity. However, it was found that more excessive and denser talc cover does not affect quality of scanning results and therefore it is not a necessity in order to achieve reliable measurements. Although good results the application of talc spray on each single specimen would be too labour-intensive, thus another method had to be developed which was fast and efficient enough to receive satisfactory surface information. Therefore, it was decided to use yellow masking tape (Fig. 5a) which provided satisfactory measurement results with average intensity of 0.36 (Fig. 5b), where talc spray was allowing to achieve 0.56 (Fig. 5c). Despite the lower intensity of the results obtained, the collected point cloud allows for reliable reconstruction of the sample surface and for further analysis. Therefore, the latter method (masking tape) presented was used for further testing as the most efficient and suitable (Fig. 6b).

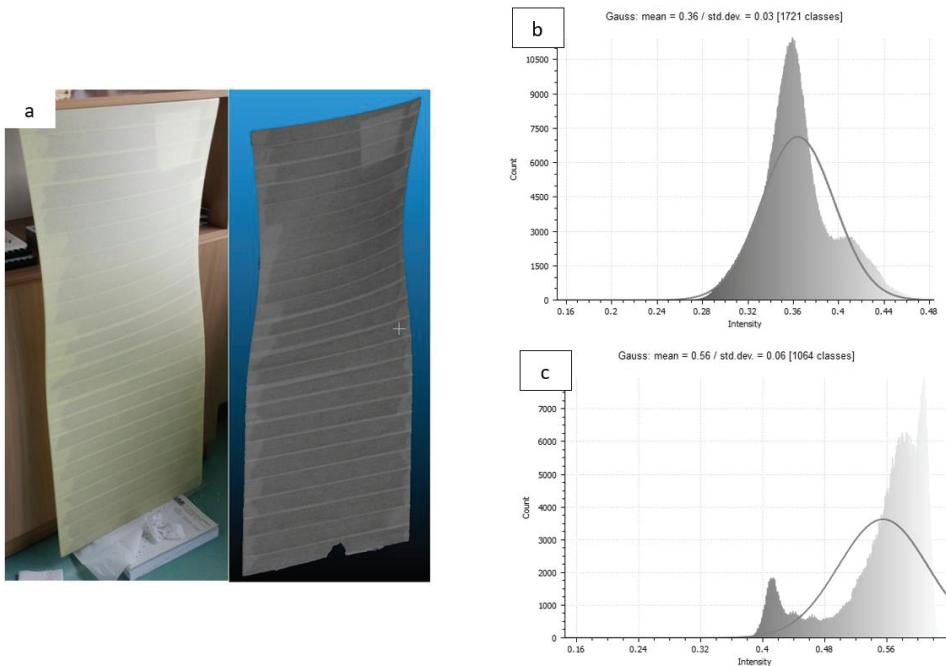


Fig. 5 a) The same sample with full-surface masking tape instead of talc spray (on the left) and received 3D scan with 2.93M points (on the right) b) Gauss distribution of intensity with mean value of 0.36 for glass surface covered with masking tape c) Gauss distribution of intensity with mean value of 0.56 for surface covered with talc spray

### 3. RESULTS AND DISCUSSION

#### 3.1. SINGLE GLASS PLY MEASUREMENT

The developed laser scanning methodology was used to 3D scan of the sample shown in Fig. 4a and further it was compared using CloudCompare software with its conceptual geometry developed in Rhino environment. It was done by isolating glass piece out of scanned region and reducing the noises using S.O.R. function (Statistical Outlier Removal). Afterwards, the genuine 3D model was imported, it was converted into point cloud and then aligned with the scanned results. Next, the distance cloud/cloud was computed and rendered in colour scale. Fig. 6a presents the results of this analysis. As can be seen, the discrepancy between Rhino model and real geometry changes on its surface and the values of these changes are not equal. These discrepancies are both positive and negative i.e. scanned surface project above and below designed 3D surface. The spectrum of these values varies from +3 mm to -2 mm. These values are not deviating from standard glass fabrication tolerances [25] and is unlikely that will cause issues during the installation. Furthermore, it could be even potentially considered as satisfactory if the scale of the individual pieces of glass on the facade is taken as an example (maximum 2,4 m × 3,2 m [7]). However, these results from comparison between real and originally intended free-form shape of the sample indicates the need for a better understanding of the slumping process itself and the reasons for the irregular upward/downward deformation of the sample. In addition, deformations do not have the same form, because each individual designed shape can lead to different forms of distortion. As augmented above, for better slumping process understanding, an idea of conducting additional experimental tests with a larger number of small samples that are evenly distributed in the furnace, was born. The assumptions of the test were clearly defined and aimed at checking which of the main aspects of production process have the greatest impact on final outcome. As a result of tracking individual stages of the process and the characteristics of glass as a material, the most important aspects that have been examined are potentially the temperature development in the furnace, the geometry of the sample itself and the location of the sample in the furnace chamber. These aspects are investigated in the main part of the paper.

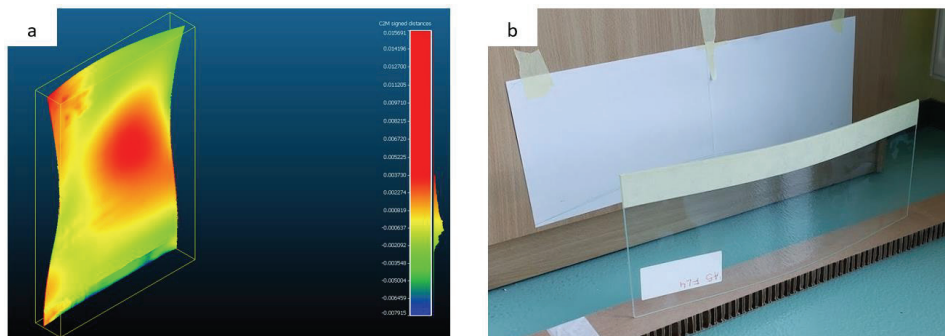


Fig. 6 a) Scanned point cloud of sample described in 3.1 aligned with designed 3D model. Magnitude of deviations is rendered in color scale on the right b) Sample from experiment described in section 3.2 prepared for 3D scanning with masking tape covering upper edge

### 3.2. EXPERIMENTAL ANALYSIS

In order to investigate the influence of defined parameters on the final shape of free-form samples a detailed experimental campaign was designed. The first step of the process was to set an appropriate temperature curve that would represent the same conditions as in the furnace during serial production. As driven parameters were chosen the rate of temperature increase, maximum values of temperature, the duration of temperature retention and, most importantly, the lowering of the temperature as a result of the furnace cooling be as close as possible to the standard procedure. A typical temperature curve can vary depending on the geometry and composition of the glass. In this case, the curve was marginally simplified, i.e. the temperature increment was set to possibly linear. The heating of the chamber depends on the furnace design. In this case the heaters were mounted on the top of the heating chamber, so their arrangement allowed for uniform exposure for radiation of the whole chamber. In addition, each heater is equipped with a separate thermocouple, which allowed for continuous control of the temperature and possible on the spot correction. Another aspect was the choice of sample geometry. It was important that the specimens were uniformly distributed in the furnace and supported in the same way - as simply supported set-up. In addition, and for later testing purposes, the glass sheets were divided into different groups according to their thickness. The remaining dimensions such as length, width and spacing on the supports were the same. During testing, the furnace, racks and all other devices were the same as those used in serial production. This was also to ensure that the parameters were as close to the original conditions as possible.

Table 1. List of samples

Sheet size	Glass thickness	Test run	Amount
500 mm x 200 mm	4 mm	1	5
500 mm x 200 mm	5 mm	1	5
500 mm x 200 mm	6 mm	1	5
500 mm x 200 mm	8 mm	1	5
500 mm x 200 mm	10 mm	1	5
500 mm x 200 mm	12 mm	1	5
<b>Sum</b>			<b>30</b>

Fig. 7a shows a typical specimen set-up used in the study. The outer dimensions of a specimen were 200 mm × 500 mm. The thicknesses of the individual sample groups have been selected to use the most common thicknesses used for facades, such as 4 mm, 5 mm, 6 mm, 8 mm, 10 mm and 12 mm Tab. 1. It is worth to mention that edges of the tested glass sheets were a raw cut flat edge with seamed corners. In total, 30 samples were used, which then all were further analysed. Glass samples were placed in heating furnace at specially prepared standers made of ceramic resistant to high temperatures. It has ensured symmetrical support and exposure to heating coils throughout the test. Fig. 7b presents several samples placed at supports with thermocouples installed to read the temperature at few significant spots like above (TC11) and below sample (TC9), between standers (TC10) and at the bottom of furnace (TC12).

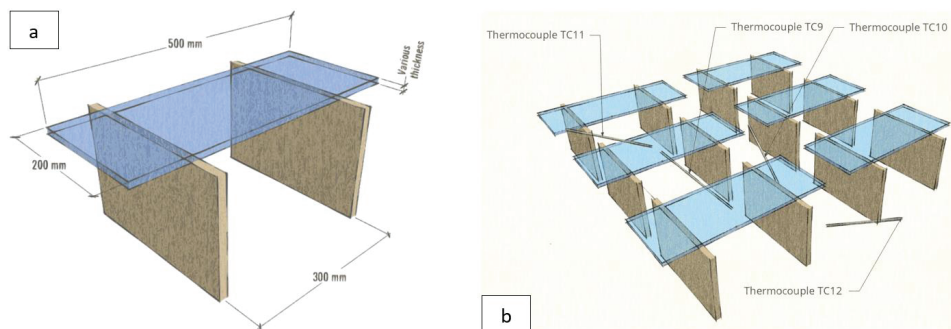


Fig. 7 a) Single sample setup b) Schematic layout of the samples together with thermocouples location

After mounting the samples in the furnace, the heating of the furnace was performed according to the heating scheme programmed in the same way as for the regular products. The furnace manufacturer has suggested this as a basic temperature curve based on their experience. However, as earlier tests

have shown, there is no universal curve and it should be adjusted to the size of the glass and its thickness. Time-temperature curve was designed to reach the temperature slightly above the glass transition temperature in slow pace and kept stabilized at 590°C degrees for 15 minutes to achieve visible sagging of the glass. Next, furnace started to cool down slowly to 100°C as can be seen in Fig. 8a. Temperature was constantly measured by 6 thermocouples at various locations of furnace (Fig. 8b) connected to multi-controller Simex MultiCon CMC-99 measuring temperature each 30 seconds of the slumping process. Thermocouples shown in Fig. 7b are the one whose results were used for further analysis, because they provided the largest amount of information about temperature development and their position in the furnace allowed for the discovery of significant differences in measurements.

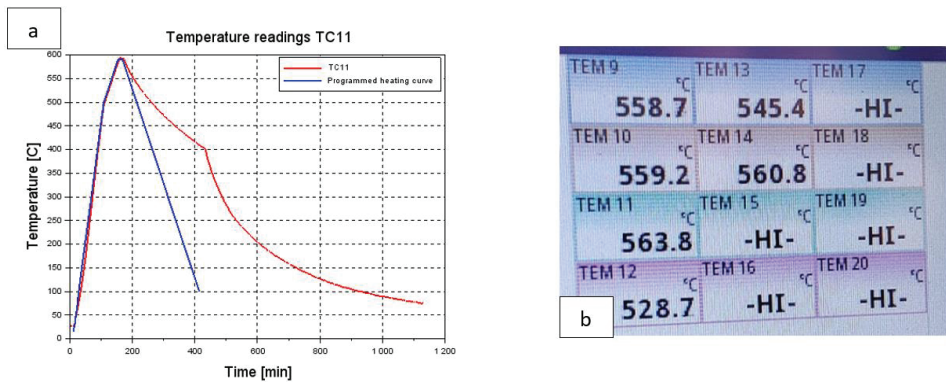


Fig. 8 a) Temperature reading of thermocouple TC11 in comparison to programmed heating curve b) Thermocouples readings on the screen of multi-controller Simex MultiCon CMC-99

### 3.3. DEFORMATION ANALYSIS

After the tests, the samples were collected and labelled according to their position in the furnace. Next, an important step was to scan the samples correctly so that the surface of the glass can be reconstructed to the required accuracy. As described in Sect. 2.2 with as numerous samples as this, the best method was to place the masking tape strip on the top edge of the sample. This method allowed for a quick and accurate scan of all the samples. As described also, each of received scanned images has been further processed in scanner's software SurphExpress and open-source CloudCompare. The aim was to obtain a real representation of the edge of the sample so that it was

possible to calculate the deflection generated during the test (mid-span downward deflection). By having the same dimensions (and thicknesses) of the samples together with the same boundary conditions, it was possible to compare the deformed samples of the same thickness and in relation to their location in the furnace.

Table 2. Measurements results

Thickness [mm]	Max [mm]	Min [mm]	Difference [mm]	Mean Value [mm]	SD [mm]
4 mm	32,77	25,18	7,59	29,67	2,96
5 mm	26,10	21,10	5,00	24,28	2,19
6 mm	22,02	16,60	5,42	19,35	2,30
8 mm	12,69	8,38	4,31	10,72	1,74
10 mm	8,03	4,72	2,31	6,18	0,88
12 mm	3,77	3,26	0,51	3,59	0,19

Fig. 9b the image shows what value was measured by a 3D scan. This is the largest distance (mostly in the centre) to the line connecting the two edges. Fig. 9b shows 5 mm thick sample immediately after the test. As an example, Fig. 10 shows scan result summary for five pieces of 4 mm glass samples, where each sample was scanned, the point cloud processed in CloudCompare and then compared with other samples with the same thickness. A thorough analysis of the results for specific thicknesses showed that the measured deflections differ significantly for samples of the same thickness.

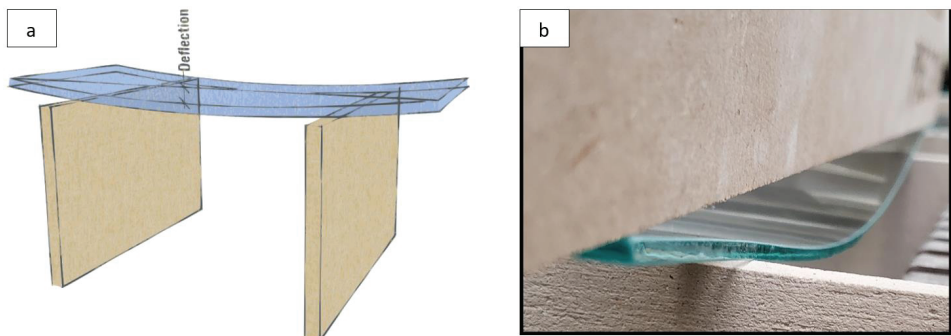


Fig. 9 a) Schematic representation how downward deflection was measured b) Glass samples of 5 mm thickness at supports after the test. It can be seen how glass sagged

Table 2 presents the results of measurements for individual test samples with such values as maximum and minimum measurement, the difference between them and the mean value of the measurement. As already mentioned, the deflection values will vary for samples of the same thickness and it was shown from the results obtained that these differences decrease as the sample thickness increases. As discussed above, the deflection values will vary for samples of the same thickness and it was shown from the results obtained that these differences decrease as the sample thickness increases. This trend can be explained by the fact that the volume of the sample increases several times faster than its surface, while maintaining the same external dimensions. The increase in volume between the thickest 12 mm glass sheet and the thinnest 4 mm is almost 3 times, while at the same time the total area increased by only 5.5%. This means that a thicker probe needs more energy to be heated and can be more resistant to short temperature fluctuations in the furnace, making heating and deformation growth more uniform. It is worth noting that the shape of the deflection curve of each of the test pieces is comparable, i.e. the highest values occur in the middle of the test specimen on a different scale. The result obtained helped to confirm that the deformation of the samples in the furnace was carried out in an unaffected manner according to the assumptions (bending of the simple beam).

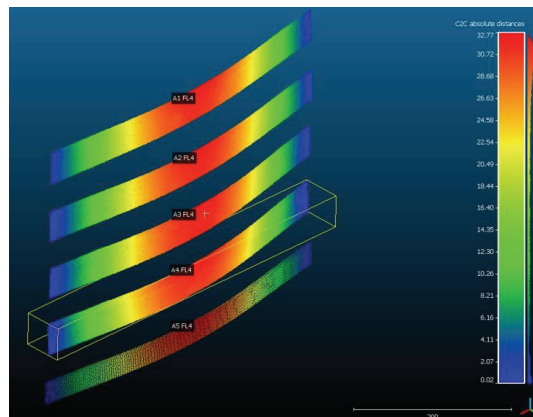


Fig. 10 Five 3D scans of 4 mm specimens processed in CloudCompare compared with max. 32,77 mm downward deflection

### 3.4. DISCUSSION

The first part of the study was focused on measuring all the samples, analysing the point clouds and comparing the obtained results among the samples of the same thickness (Fig. 11a). In the next stage it was investigated that the samples deflected equally in value to what the test was designed. Nevertheless, the test showed significant differences between the samples of the same thickness as can be seen in the table presented in Fig. 11b. The measured deflections for the individual sheets were applied to the matrix which was a schematic view of the furnace chamber. The values in the individual cells have been formatted in such a way that the colour scale changes individually for each type of glass thickness. This allowed us to observe that regardless of the thickness of the sample, the deflection scale changes on the furnace plan. The obvious reason for such a significant discrepancy could be a variable distance between the supports, but they have been checked with great caution to ensure that all samples have the same support. The resulting image rendered that the samples placed closer to the wall of the furnace showed a lower value of sagging and this was the case for all types of glass with different thicknesses. This effect can be explained by the fact that during the test, the samples were not heated equally and did not reach the same temperature and one place in the centre of the furnace became more heated thus resulted in a higher deformation, while the others were located closer to the wall of the furnace where temperature was lower, thus the deformation was smaller. This observation indicates a non-homogeneous heat distribution inside the furnace. This conclusion finds support in the readings obtained from thermocouples.

a		Furnace wall					
F u r n a c e		FL4 - 25.18	FL5 - 21.1	FL6 - 18.11	FL8 - 8.38	F u r n a c e	
		FL4 - 28.96	FL5 - 24.8	FL6 - 21.43	FL8 - 9.54		
		FL4 - 31.83	FL5 - 25.1	FL6 - 22.02	FL10 - 6.65		
		FL4 - 32.77	FL5 - 26.1	FL8 - 12.69	FL10 - 7.03		
		FL4 - 29.63	FL6 - 18.6	FL8 - 11.82	FL10 - 6.23		
w a l l		FL5 -	FL6 - 16.6	FL8 - 11.16	FL10 - 6.26		
					FL10 - 4.72		
					FL12 - 3.68		
					FL12 - 3.66		
					FL12 - 3.58		
		Furnace wall					

b		Furnace wall					
F u r n a c e		25,18	21,1	18,11	8,38	F u r n a c e	
		28,96	24,8	21,43	9,54		
		31,83	25,1	22,02	6,65		
		32,77	26,1	12,69	7,03		
		29,63	18,6	11,82	6,23		
w a l l			16,6	11,16	6,26		
					4,72		
					3,68		
					3,66		
					3,58		
		Furnace wall					

Fig. 11 a) The layout being schematic representation of furnace plan with value for downward deflection for each single glass sheet e.g. left upper corner is glass sample 4 mm thick with 25.18 mm downward deflection b) The same layout showed in the Fig. 11a with different formatting which is showing values for downward deflection with color range representing maximum values (towards full green) and minimum values (towards full yellow) per single glass thickness

The first objective was to check how the temperature in the furnace developed in comparison with the pre-set heating curve. Due to the limited number of temperature's measuring points, it is not possible to reproduce the exact temperature distribution throughout the furnace volume. For this reason, further analysis consisted of analysing the readings from specific thermocouples and trying to trace how the temperature was changing during the test. Fig. 8a shows the reading from the TC11 thermocouple in comparison to the set heating profile. This TC11 was selected (it was placed in the middle of the furnace at the height of the samples), because it showed the measurements closest to the expected development of the temperature. After a more detailed analysis of the data, the reading of the thermocouple diverged from the instantaneous reading on the thermocouples installed in the furnace by about 7°C and equalised after about 4 minutes. This shows a certain inertia of the furnace, but these values for the top-mounted thermocouple (TC11) are low that have no effect on the process. This is different for other thermocouples that are not directly exposed to the heating elements. The next step was to analyse how the temperature development in other areas was progressing and the data from the remaining thermocouples were analysed and compared with each other. It turned out that the temperatures on particular thermocouples differ significantly in relation to each other and the greatest differences were observed for the thermocouple TC12 placed on the bottom of the furnace and the TC10 placed just under the samples. Both thermocouples were underneath the test samples and isolated from the heating elements. These differences can be as high as 149°C (TC12) and 128°C (TC10) as shown on the graph (Fig. 12). The biggest differences occurred in the first phase when the temperature rise was intense and was rapid (96 minutes to reach 500°C with a starting point of 20°C and increment 5°C per minute). After that time, the increment was reduced to 2°C per minute for another 45 minutes. This resulted that the earlier recorded differences starting to decrease quickly. So, it can be concluded that the original increment occurred at a rate too rapid for the temperature to be equal in the volume of the furnace. Another worthy observation is that two earlier mentioned thermocouples reached much lower temperatures than TC11, i.e. TC10  $T_{max}=573^{\circ}\text{C}$  and TC12  $T_{max}=560^{\circ}\text{C}$ . This means that the above temperatures are below the approximate glass transition temperature, which, in direct correlation, has the effect of sagging of the glass, once it will not reach the required temperature to start deforming under gravity alone. The next temperature jump on the chart is caused by partial opening of the furnace cover after about 95 minutes of cooling from 590°C to 400°C. As can be seen, this has a large impact on the temperature distribution in the furnace, because it is a sudden jump of almost 58°C, which then only starts to recover after 200 minutes. Such a rapid change in temperature can affect the process of slow cooling (annealing) to avoid residual stress concentrations within the glass. Due to the complexity of the process and the initial

measurements, the test proved to contain a number of limitations. The main constrain of the experiments is the number of thermocouples and temperature reading points, thus it was not possible to investigate air temperature variation within entire chamber's volume. This could help to understand how the hot air is circulating within the chamber and how glass itself is impacting the airflow. In addition, the temperature was measured for the air surrounding the specimens and not for the glass sheet itself. Therefore, it is not entirely known how the temperature developed inside the glass sheet and it can be only assumed that the temperature oscillated around the thermocouple readings. Another limit was that it was not possible to measure continuously deformation of each of the sample thicknesses in relation to the time-temperature. Such measurement would require sensors placed in the furnace chamber throughout the entire heating process. These devices must be able to withstand the temperatures and transmit information outside the furnace. To our current state of knowledge, such a device is not yet available. It is possible to measure by analysing the image from a cooled camera placed inside the chamber or alternative exterior device in place in the chamber and recording the image through the viewfinder. In this case, such a camera was not available and its use would require a partial modification of the furnace.

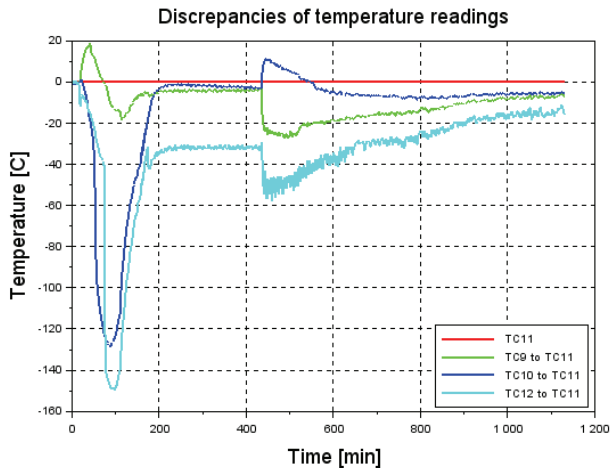


Fig. 12 Temperature deviations for different thermocouples in comparison to thermocouple TC11

## 4. CONCLUSIONS

The findings confirm that entire slumping process is extremely complex task driven not only by material properties of the glass, but also strongly by conditions which are occurring in furnace's chamber. Hot air distribution plays significant role in uniformity of heating the glass lite. Size and shape of the glass, as well as mould, can impact significantly the slumping process once they are creating obstacles for heated air leading to formulation of steady air zones with elevated temperature. This could explain why the samples placed in the middle of the furnace showed a higher deformation than the others. In mass production and for larger glass panes, this could cause some regions of the bent glass to deform more than the rest, with the result that the designed geometry would not be achieved. An additional problem resulting from this unbalanced heating may be that the edges of the panel will heat up much faster than the centre and may also result in undesirable excessive distortion. Additionally, for larger glass panes, it can lead to an unbalanced distribution of residual stresses, which can cause inhomogeneous stress state and be more vulnerable to breakage due to external loading (both mechanical and thermal). These observations could explain why the previously scanned samples did not fully fit into the Rhino model. Further work will be needed to focus on improving the air circulation in the furnace chamber. In order to develop the most efficient solution, a computational fluid dynamics (CFD) modelling techniques can be used to simulate the distribution of the hot air and the influence of elements such as the glass panel, rack, mould placed in the furnace. This approach may definitely save the high cost of prototyping solutions. Subsequently, it will be necessary to modify the furnace and carry out exactly the same test as described in this article to compare the results and assess the effectiveness of the new solution. For the next test, it will be necessary to develop a method that will allow for the continuous measurement of the deformation over time. This will allow the temperature to correlate with the growth of the deformation and, after conversion, to obtain results representing how rheological parameters for soda-lime-silica glass changes in relation to temperature. Also, the glass scanning method developed for these tests has proven to be an effective and reliable way of measuring the glass surface. This method can be successfully used to scan larger samples and the methodology of comparing the resultant glass pane into the established 3D model can be a good method to optimize production and improve the quality of the end product. Since the process of producing such glass is almost every time an individualized and more time-consuming process than the production of flat glass, using a 3D laser on the production line could be another quality control tool. Nevertheless, there is a series of issues that still need to be solved, such as scanning. In addition, the process of data analysis from the scanner and 3D model

comparison needs to be automated in order to run more efficiently and produce results on the production line, so that the furnace operator can adjust the process on the spot without the need for a second person analysing data in the office and awaiting for the results.

## 5. ACKNOWLEDGMENTS

The authors greatly appreciate the support by the company Press Glass S.A. which provided its testing furnace, samples, equipment and contributed with their experience to the article.

## REFERENCES

- [1] L. Corbusier, P. Stirton and T. Benton, "Glass, the Fundamental Material of Modern Architecture," West 86th: A Journal of Decorative Arts, Design History, and Material Culture, 2012.
- [2] F. Oikonomopoulou, T. Bristogianni, L. Barou, F. Veer and R. Nijse, "The potential of cast glass in structural applications. Lessons learned from large-scale castings and state-of-the art load-bearing cast glass in architecture," Journal of Building Engineering, 2018.
- [3] Y. Chen, Thermal Forming Process for Precision Freeform Optical Mirrors and Micro Glass Optics, 2010.
- [4] B. Ananthasayanam, Computational Modeling Of Precision Molding Of Aspheric Glass Optics, Clemson University, 2008.
- [5] J. H. Nielsen, Tempered Glass: Bolted Connections and Related Problems, Technical University of Denmark (DTU), 2009.
- [6] J. Neugebauer, "Applications for Curved Glass," in COST Action TU0905, Mid-term Conference on Structural Glass, 2013.
- [7] T. Fildhuth and J. Knippers, "Considerations Using Curved , Heat or Cold Bent Glass for Assembling Full Glass Shells," engineered transparency. International Conference at glasstec, 2012.
- [8] T. Kopic, I. Svetel and Z. Cekic, "Complexity of Curved Glass Structures," in IOP Conference Series: Materials Science and Engineering, 2017.
- [9] O. Enghardt, "Advanced building skins," in Proceedings of the International Conference on Building Envelope Design and Technology, Graz, 2015.
- [10] J. Bijster, C. Noteboom and M. Eekhout, "Glass Entrance Van Gogh Museum Amsterdam," Glass Structures & Engineering, 2016.
- [11] P. Block, J. Knippers, N. J. Mitra and W. Wang, Advances in Architectural Geometry 2014, Springer Publishing Company, Incorporated, 2014.
- [12] C. Gengnagel, O. Baverel, J. Burry, M. R. Thomsen and S. Weinzierl, Impact: Design With All Senses, Springer International Publishing, 2020.
- [13] H. Pottmann, A. Schiftner, P. Bo, H. Schmiedhofer, W. Wang, N. Baldassini and J. Wallner, "Freeform surfaces from single curved panels," ACM SIGGRAPH 2008 papers on - SIGGRAPH '08, 2008.
- [14] D. R. Shelden, Digital Surface Representation and the Constructibility of Gehry' s Architecture, MIT, 2002.
- [15] M. Stavric, M. Manahl and A. Wiltsche, "Discretization of double curved surface," in Challenging Glass 4 & COST Action TU0905 Final Conference, 2014.
- [16] U. Knaack, T. Klein, M. Bilow and H. Techen, Performance driven envelopes, Rotterdam: 010 Publishers, 2011.
- [17] M. Eigensatz, M. Deuss, A. Schiftner, M. Kilian, N. J. Mitra, H. Pottmann and M. Pauly, "4. Case Studies in Cost-Optimized Paneling of Architectural Freeform Surfaces," Advances in Architectural Geometry , 2016.
- [18] F. Ensslen, J. Schneider and S. Schula, "Produktion, Eigenschaften und Tragverhalten von thermisch gebogenen Floatgläsern fuer das Bauwesen - Erstpruefung und werkseigene Produktionskontrolle im Rahmen des Zulassungsverfahrens," Stahlbau, 2010.
- [19] Y. Chen and A. Y. Yi, "Design and fabrication of freeform glass concentrating mirrors using a high volume thermal slumping process," Solar Energy Materials and Solar Cells, 2011.
- [20] S.-J. Liu, C.-S. Chen, L.-B. Huang and R.-J. Yang, "Method For Manufacturing Curved Glass Sheet And Mold Employed In The Same". Patent US8448470B2, 2013.

- [21] M. Feijen, I. Vrouwe and P. Thun, "Cold-bent single curved glass; opportunities and challenges in freeform facades," in *Challenging Glass 3: Conference on Architectural and Structural Applications of Glass*, 2012.
- [22] I. Basis Software, "SurphExpress," 2019. [Online]. Available: <http://www.surphaser.com/>.
- [23] CloudCompare, "CloudCompare (version 2.10.2)," 2019. [Online]. Available: <http://www.cloudcompare.org/>.
- [24] N. Pfeifer, P. Dorninger, A. Haring and H. Fan, "Investigating terrestrial laser scanning intensity data: quality and functional relations," in *8th Conference on Optical 3-D Measurement Techniques*, 2007.
- [25] Press Glass SA, *Press Glass - Company Standard*, Press Glass SA, 2016.

## LIST OF FIGURES AND TABLES

Fig. 1 a) Mixed Use Development Balna in Budapest by ONL (source: <https://www.oosterhuis.nl/>) b) Prada Aoyama in Tokyo by Herzog and de Meuron (source: <https://www.herzogdemeuron.com/>)

Rys. 1 a) Mixed Use Development Balna w Budapeszcie zaprojektowany przez ONL (źródło: <https://www.oosterhuis.nl/>) b) Prada Aoyama w Tokio zaprojektowany przez Herzog and de Meuron (źródło: <https://www.herzogdemeuron.com/>)

Fig. 2 Renovation of Nordstan Shopping Centre facade in Sweden

Rys. 2 Renowacja centrum handlowego Nordstan w Szwecji

Fig. 3 a) Glass samples at racks b) 3D laser scanner SURPHASER 100HSX used for the experiment

Rys. 3 a) Próbkki szkła na stojaku b) Skaner 3D SURPHASER 100HSX użyty w trakcie eksperymentu

Fig. 4 a) Prepared sample with sprayed talc (on the left) and isolated point cloud from the 3D scan in

CloudCompare (on the right) b) Intensity of scanned point cloud shown as grey-scale in CloudCompare software for single glass sample

Rys. 4 a) Przygotowana próbka pokryta talkiem (po lewej) i wyizolowana chmura punktów ze skanu 3D w programie CloudCompare (po prawej) b) Gęstość otrzymanej chmury punktów przedstawiona w skali szarości w programie CloudCompare dla pojedynczej tafli szkła

Fig. 5 a) The same sample with full-surface masking tape instead of talc spray (on the left) and received 3D scan with 2.93M points (on the right) b) Gauss distribution of intensity with mean value of 0.36 for glass surface covered with masking tape c) Gauss distribution of intensity with mean value of 0.56 for surface covered with talc spray

Rys. 5 a) Ta sama próbka pokryta w całości taśmą zamiast talku technicznego (po lewej) i otrzymany skan 3D z ilością 2,93 milionów punktów (po prawej) b) Rozkład Gaussa gęstości chmury punktów z wartością średnią 0,36 dla szkła pokrytego taśmą c) Rozkład Gaussa gęstości chmury punktów z wartością średnią 0,56 dla szkła pokrytego talkiem

Fig. 6 a) Scanned point cloud of sample described in 3.1 aligned with designed 3D model. Magnitude of deviations is rendered in color scale on the right b) Sample from experiment described in section 3.2 prepared for 3D scanning with masking tape covering upper edge

Rys. 6 a) Otrzymana chmura punktów próbki opisanej w rozdziale 3.1 porównana ze źródłowym modelem 3D. Rozmiar różnic przedstawiona w skali kolorów przedstawiona po prawej b) Próbka z eksperymentu opisanego w rozdziale 3.2. przygotowana do skanu 3D z taśmą zakrywającą górną krawędź

Fig. 7 a) Single sample setup b) Schematic layout of the samples together with thermocouples location

Rys. 7 a) Ustawienie dla jednej próbki b) Schematyczny rozkład próbek razem z położeniem termopar

Fig. 8 a) Temperature reading of thermocouple TC11 in comparison to programmed heating curve b)

Thermocouples readings on the screen of multi-controller Simex MultiCon CMC-99

Rys. 8 a) Odczyt temperatury dla termopary TC11 w porównaniu do zaprogramowanej krzywej grzania b)

Odczyt dla termopar przedstawiony na ekranie multikontrolera Simex MultiCon CMC-99

Fig. 9 a) Schematic representation how downward deflection was measured b) Glass samples of 5 mm

thickness at supports after the test. It can be seen how glass sagged

Rys. 9 a) Schematyczna reprezentacja w jaki sposób było mierzone ugięcie b) Próbka szkła o grubości 5 mm

na podporach po teście, gięcie jest wyraźnie widoczne

Fig. 10 Five 3D scans of 4 mm specimens processed in CloudCompare compared with max. 32,77 mm

downward deflection

Rys. 10 Pięć skanów 3D dla próbek o grubości 4 mm przetworzonych w programie CloudCompare i

wzajemne porównane. Maksymalne zmierzone ugięcie wynosi 32,77 mm

Fig. 11 a) The layout being schematic representation of furnace plan with value for downward deflection for

each single glass sheet e.g. left upper corner is glass sample 4 mm thick with 25.18 mm downward

deflection b) The same layout showed in the Fig. 11a with different formatting which is showing values

for downward deflection with color range representing maximum values (towards full green) and

minimum values (towards full yellow) per single glass thickness

Rys. 11 a) Rozkład będący schematyczną reprezentacją wnętrza pieca wraz informacją o ugięciu dla każdej z

próbek np. w lewym górnym narożniku jest próbka szklana o grubości 4 mm która ugięła się 25,18 mm b)

Ten sam rozkład co na Rys. 11a z innym formatowaniem pokazujący te same wartości ugięcia

reprezentowane jako skala kolorów (maksymalne wartości z pełnym kolorem zielonym, a minimalnymi

wartościami z pełnym kolorem żółtym) dla poszczególnych grubości próbek

Fig. 12 Temperature deviations for different thermocouples in comparison to thermocouple TC11

Rys. 12 Różnice w temperaturach dla różnych termopar w porównaniu do TC11

Tab. 1 List of samples

Tab. 1 Lista próbek

Tab. 2 Measurements results

Tab. 2 Wyniki pomiarów

**PRODUKCJA WIELKOWYMIAROWEGO GIĘTEGO WIELOPLASZCZYZNOWO SZKŁA ARCHITEKTONICZNEGO  
- WYZWANIA I OGRANICZENIA**

*Słowa kluczowe:* formowanie szkła, szkło gięte, nowoczesna architektura, produkcja szkła, skanowanie laserowe

**PODSUMOWANIE:**

W artykule skupiono się na rozwoju wiedzy na temat wielopłaszczyznowego gięcia na gorąco szkła architektonicznego produkowanego w procesie opadania oraz na wyzwaniach i ograniczeniach samego procesu. Ze względu na złożoność procesu, wiele czynników wpływa na końcową jakość szkła, a głównym celem było lepsze zrozumienie samej procedury w celu poprawy kontroli i jakości procesu produkcji tego typu szkła. W związku z rosnącym zainteresowaniem tego rodzaju szkłem do zastosowań architektonicznych, rynek przetwórstwa szkła coraz częściej inwestuje w wymagane technologie. W chwili obecnej ta rosnąca nisza nie ma w dostępnej literaturze wielu bezpośrednich wyjaśnień na temat zachowania się szkła w piecu, co z kolei zachęca do współpracy pomiędzy środowiskiem naukowym a producentami. W niniejszym artykule przedstawiono przeprowadzone doświadczenia, które doprowadziły do lepszego zrozumienia pracy pieca oraz wpływu poszczególnych czynników na jego funkcjonowanie. W oparciu o trójwymiarowy model numeryczny wyprodukowano dużą próbkę szkła, która następnie została zeskanowana laserem 3D metodą opracowaną na potrzeby eksperymentu. Wyniki sugerowały, że konieczny jest dokładniejszy test z wykorzystaniem pełnowymiarowego pieca. Na tej podstawie eksperyment został przeprowadzony z wykorzystaniem dużej liczby próbek szkła o różnej grubości. Wyniki eksperymentu pozwoliły lepiej zrozumieć i wykazać potrzebę dalszych badań tej technologii w celu optymalizacji jakości procesu.

Received: 14.06.2020, Revised: 07.08.2020

